Fermi National Accelerator Laboratory

FERMILAB-76/26-EXP
7500.216
7500.456

DRIFT CHAMBER SYSTEM FOR K-e SCATTERING EXPERIMENT AT FERMILAB ACCELERATOR

T. S. Nigmanov, V. P. Pugachevich, V. D. Riabtsov,
M. D. Shafranov, E. N. Tsyganov, D. V. Uralsky,
and A. S. Vodopianov
Joint Institute for Nuclear Research, Dubna, USSR

and

F. Sauli
CERN, Geneva, Switzerland

and

M. Atac and J. Tompkins
Fermi National Accelerator Laboratory, Batavia, Illinois 60510 USA

March 1976

Drift Chamber System for K-e Scattering Experiment at Fermilab Accelerator

T. S. Nigmanov, V. P. Pugachevich, V. D. Riabtsov, M. D. Shafranov,
E. N. Tsyganov, D. V. Uralsky, A. S. Vodopianov
Joint Institute for Nuclear Research, Dubna, USSR

F. Sauli
CERN, Geneva, Switzerland

M. Atac, J. Tompkins
Fermi National Accelerator Laboratory, Batavia, Illinois USA

Abstract

A drift chamber system for a K-e elastic scattering experiment is described. The experiment will be done at Fermilab using a kaon beam of 250 GeV/c. The chambers were built at JINR, Dubna, and tested at Fermilab using a pion beam of 150 GeV/c at intensities up to 5×10^5 particles per second per wire. An average spatial accuracy of 60 μm is obtained.

The construction of the chambers is similar to that of Reference 1. Wire electrodes are used to shape the electric field. The spacing of the field shaping wires is 2 mm. A resistive divider provides negative voltages at the shaping wires, while the signal wires are at positive potential. The current through a signal wire is limited by 1 MΩ resistor. Chambers of two sizes, 12.5 x 12.5 cm^2 and 25 x 25 cm^2, were constructed and tested. Individual planes are combined in modules, each module containing 4 X and 4 Y planes in one gas enclosure. The total material in a module containing eight planes is 0.141 g/cm^2 (0.008 radiation length) in the sensitive area. A 25 x 25 cm^2 module is shown in Fig. 1. The modules can be easily disassembled, allowing for easy replacement of signal wires.

The spacing of signal wires is 42 mm, so that the maximum drift length is 21 mm. The signal wires of adjacent planes are shifted by 21 mm to resolve the left-right ambiguity. Gold plated tungsten wires of 25 μm diameter are used at a tension of 50 grams. The distance between shaping electrodes and signal wires is 3 mm.

A mixture of argon (67.2%), isobutane (30.3%), and methylal (2.5%) was used.

Signals were picked up from the wires through 470 pF capacitors and 200 Ω resistors, detected by amplifier-discriminators which are located directly on the chambers. The threshold of an amplifier-discriminator is adjustable in the range of 5 to 15 μA with output signals corresponding to NIM standard.

Two modules, one 12.5 x 12.5 cm^2 and the other 25 x 25 cm^2, were placed in a beam for tests described here. The modules were separated by a distance of about one meter. Twenty signal wires in the first module and 28 wires in the second module in the beam region were activated. Therefore, the system comprised 48 signal wires.

The signal from a coincidence of two scintillation counters was used as common start for time-to-digital converters (TD811 of ORTEC-EG&G). Each digit of this TDC was 0.25 nsec with a full range of 500 nsec. Test inputs of the amplifiers were used for calibration of all channels.

A beam of negatively charged particles of 150 GeV/c momentum was used to test the drift chambers. The beam size was 20 mm (FWHM) both in X and in Y views, and the angular divergence of the beam was less than 0.06 mrad. The spill time was 0.9 sec.

Data was checked in real time by an on-line software system. Efficiencies of all planes and accuracies for each wire were calculated, and beam profiles for each wire were displayed.

Figure 2 displays an average efficiency as a function of anode voltage of the 25 x 25 cm^2 module for three different beam intensities. It shows that even at 0.5×10^6 particles per burst a reasonably high efficiency (98.2%) can be achieved by using high anode voltage and low electronics thresholds.

Track selection was done using the following criteria:

a) The times from the left and right signal wires added together appropriately to check the constancy requirement. A gaussian-like distribution was found from the added times. Those tracks falling within ± 15 nsec deviation were accepted as good candidates.

b) In order to avoid the need to measure wire-by-wire systematic corrections for this test only wires on the same side of a particle track were used in the following computation.

The spatial resolution of one wire was calculated by using reconstructed trajectories of the beam particles detected by three planes, assuming that the resolutions of all wires are equal. The root-mean-square, ϵ, of the distribution of the value

$$\delta = t_2 - t_1 - (t_3 - t_1) \cdot (Z_2 - Z_1)/(Z_3 - Z_1)$$

is related to the spatial accuracy of one wire by the expression

$$\sigma = \epsilon \cdot v/\sqrt{2}\,(1 - DZ + (DZ)^2)\ ,$$

in which t_1, t_2, t_3 are the drift times, Z_1, Z_2, Z_3 the z-positions of the wire planes, v the drift velocity, and $DZ = (Z_2 - Z_1)/(Z_3 - Z_1)$. ϵ was obtained by fitting the δ-distribution to a gaussian form. Figure 3 shows σ vs drift length for the 25 x 25 cm^2 module at low beam intensity (several thousand particles per burst), at an anode voltage +1.75 kV. The solid curve is fit by the expression

$$\sigma = \sqrt{n} \cdot I_o^{-1} \cdot \sin \text{arctg}\,(n/I_o \cdot X) + B \cdot X^{1/2} + C,$$

in which the first term describes dispersion due to fluctuations in the time of arrival of nth electron causing the output signal from the amplifier, I_o being a density of primary ionization clusters; the second term describes diffusion processes, and the third term describes fluctuations due to electronics (time slewing, etc.). The average value of the spatial resolution from Fig. 3 is equal to 59 μm. This result is slightly better than in References 1 and 2 and may be due to more precise readout electronics, lower amplifier thresholds, and less multiple Coulomb scattering.

The spatial resolution with respect to anode voltage was investigated. Figure 4 shows the data as a group of fitted curves describing accuracy as a function of the drift length for different anode voltages. The average accuracy relative to anode voltage is shown in Fig. 5.

Investigation of spatial resolution vs beam intensity was also carried out. Figure 6 shows the average accuracy of the drift chambers at different intensities using the same anode voltage of + 1.75 kV. The average accuracy degrades to 85 μm at 0.5×10^6 particles per burst. It is approximately equivalent to a decrease in anode voltage of 200 V. The average accuracy is 81 μm at this intensity at an anode voltage of + 1.85 kV.

The authors would like to specifically acknowledge the support of UCLA, the Fermilab directorate, and the JINR, Dubna, in this effort.

REFERENCES

1. G. Charpak et al., Nucl. Instrum. Methods 108, 413 (1973).

A. Breskin et al., Nucl. Instrum. Methods 119, 9 (1974).

A. Breskin et al., Nucl. Instrum. Methods 124, 189 (1975).

2. M. Atac and C. Ankenbrandt, IEEE Transactions on Nuclear Science, Vol. NS-22, February 1975.

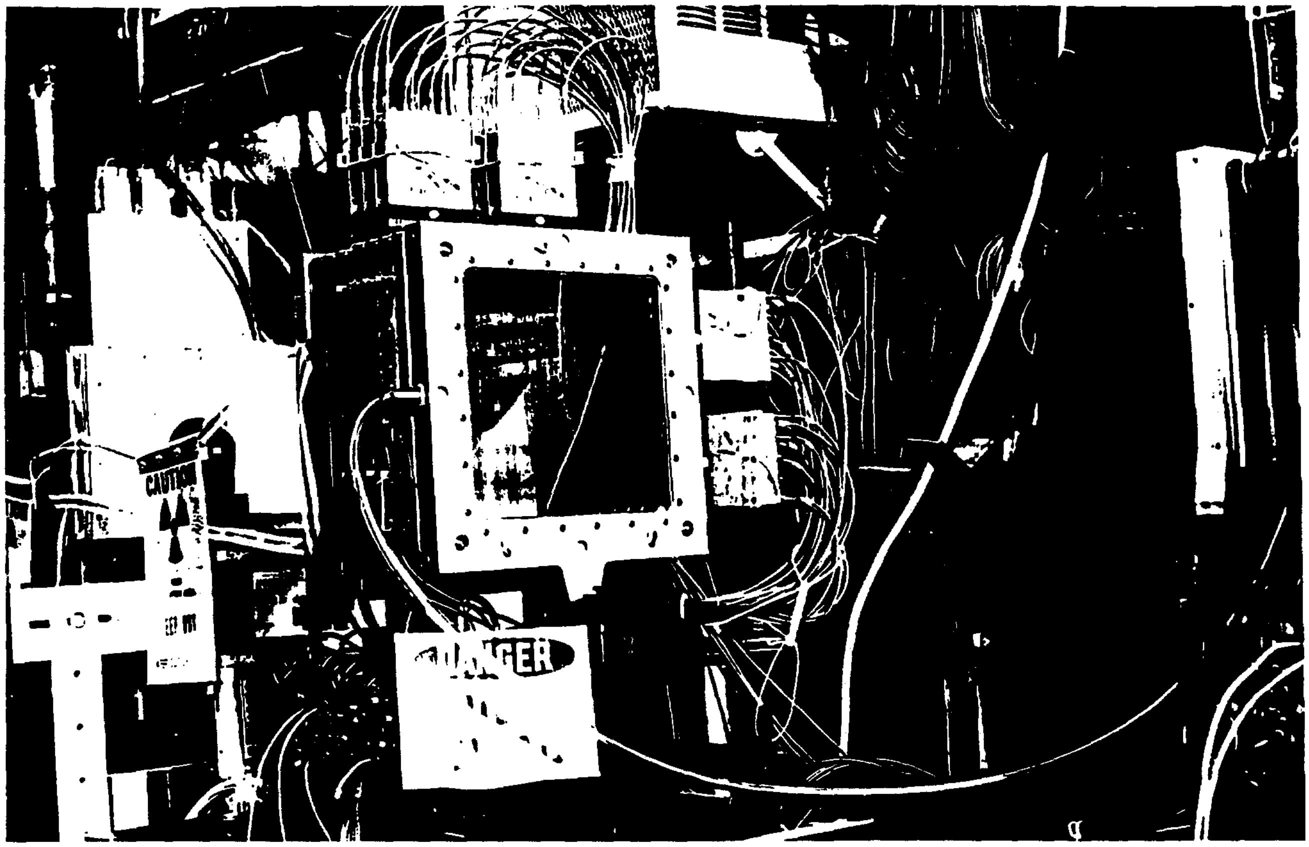

Fig. 1. Drift chamber module of 25×25 cm^2 size.

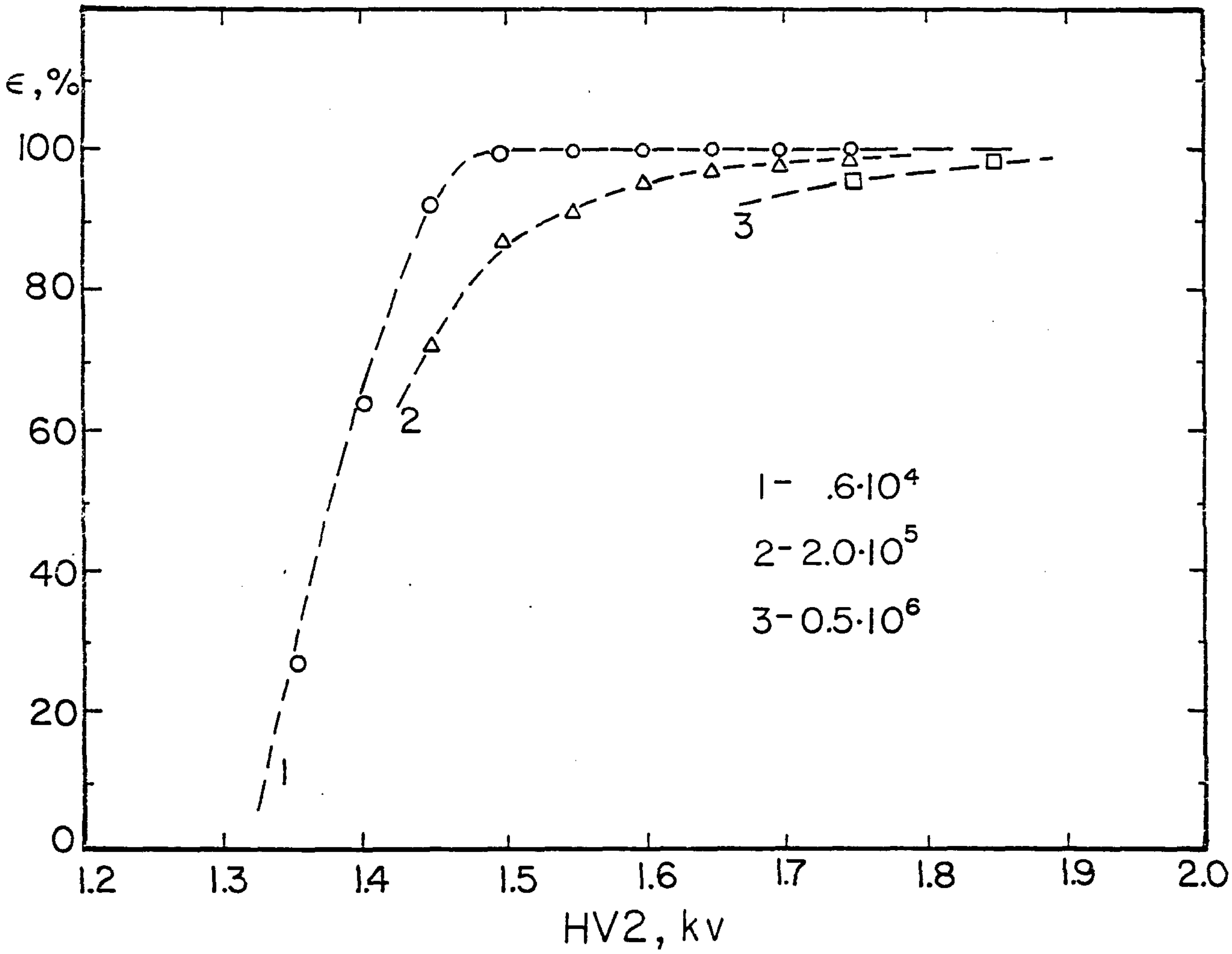

Fig. 2. Average efficiency of drift chambers vs anode voltage. Curve 1 for data at an intensity of 6×10^3 particles per burst; Curve 2, 2×10^5; Curve 3, 0.5×10^6.

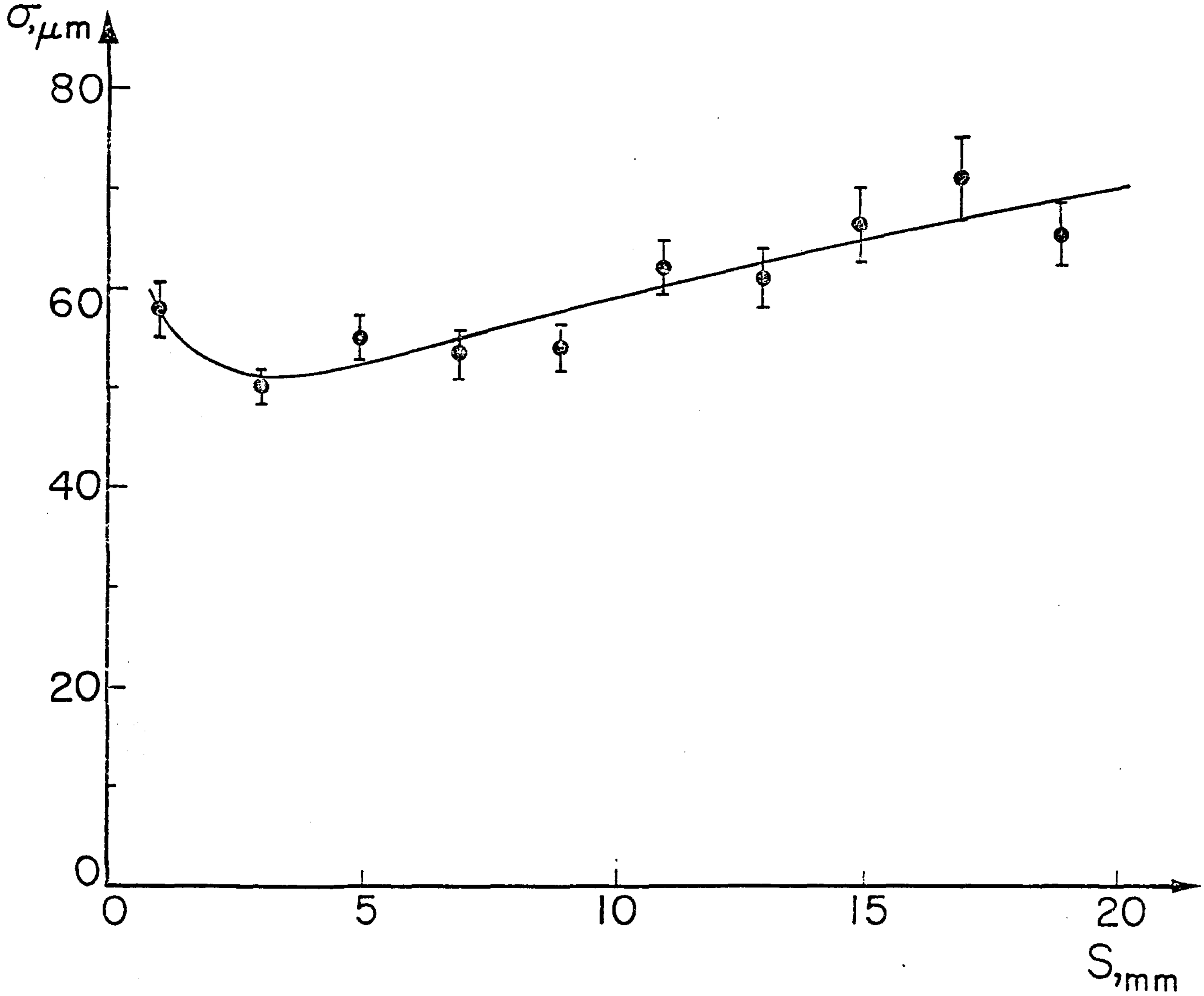

Fig. 3. Spatial resolution of drift chambers vs drift length at low intensity.

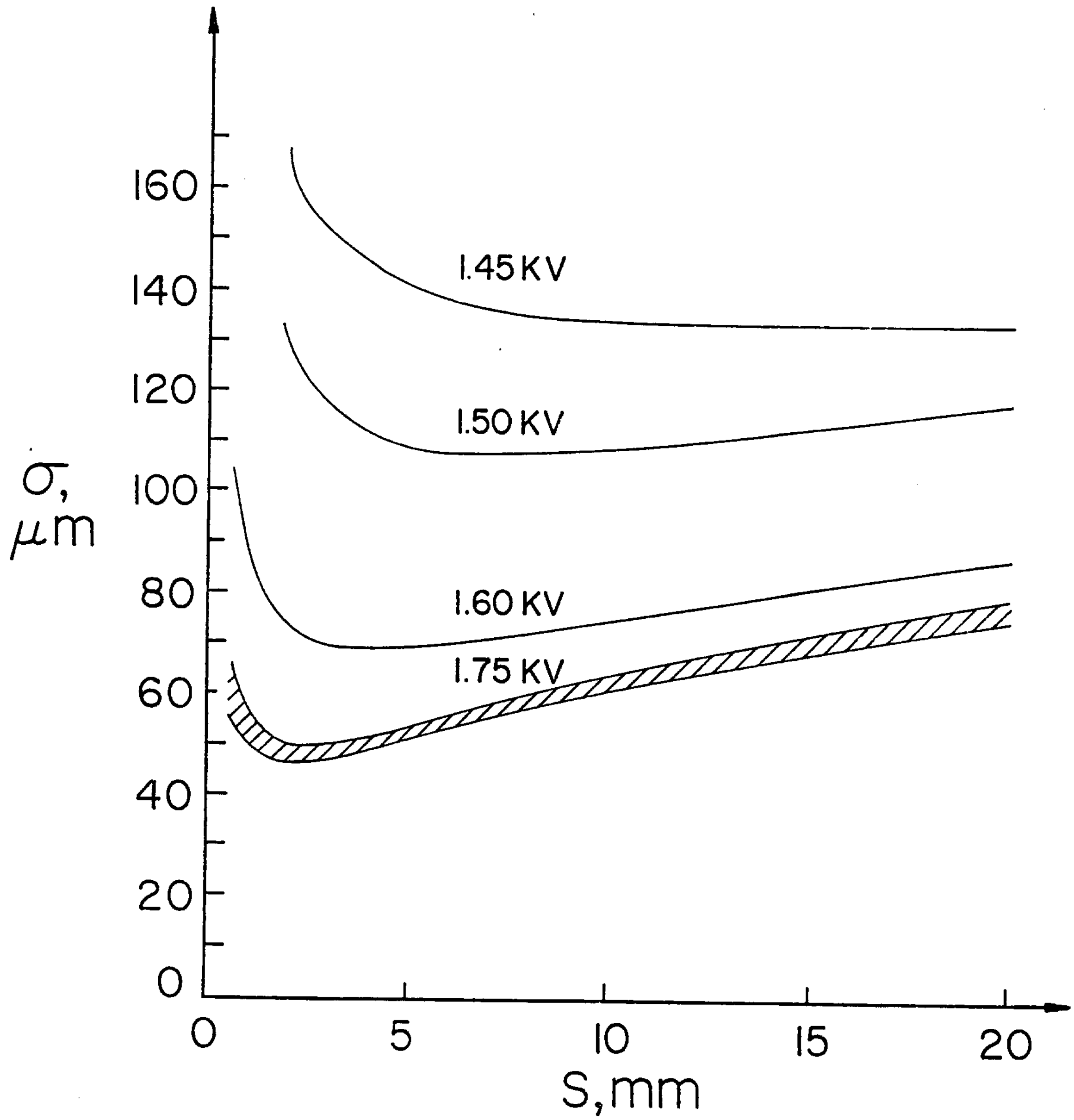

Fig. 4. Curves of spatial resolution of drift chambers vs anode voltage at low intensity.

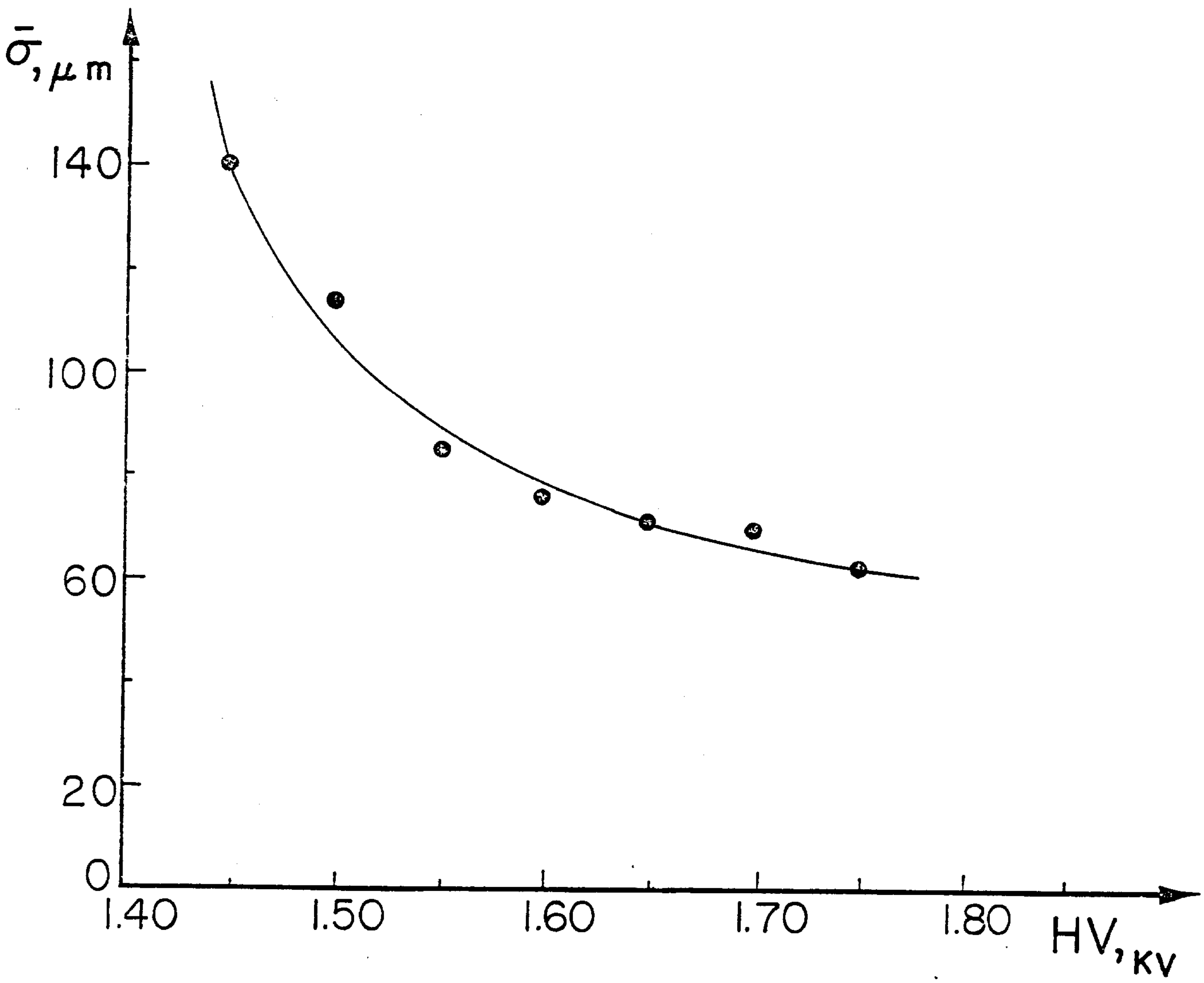

Fig. 5. Average spatial accuracy of drift chambers vs anode voltage.

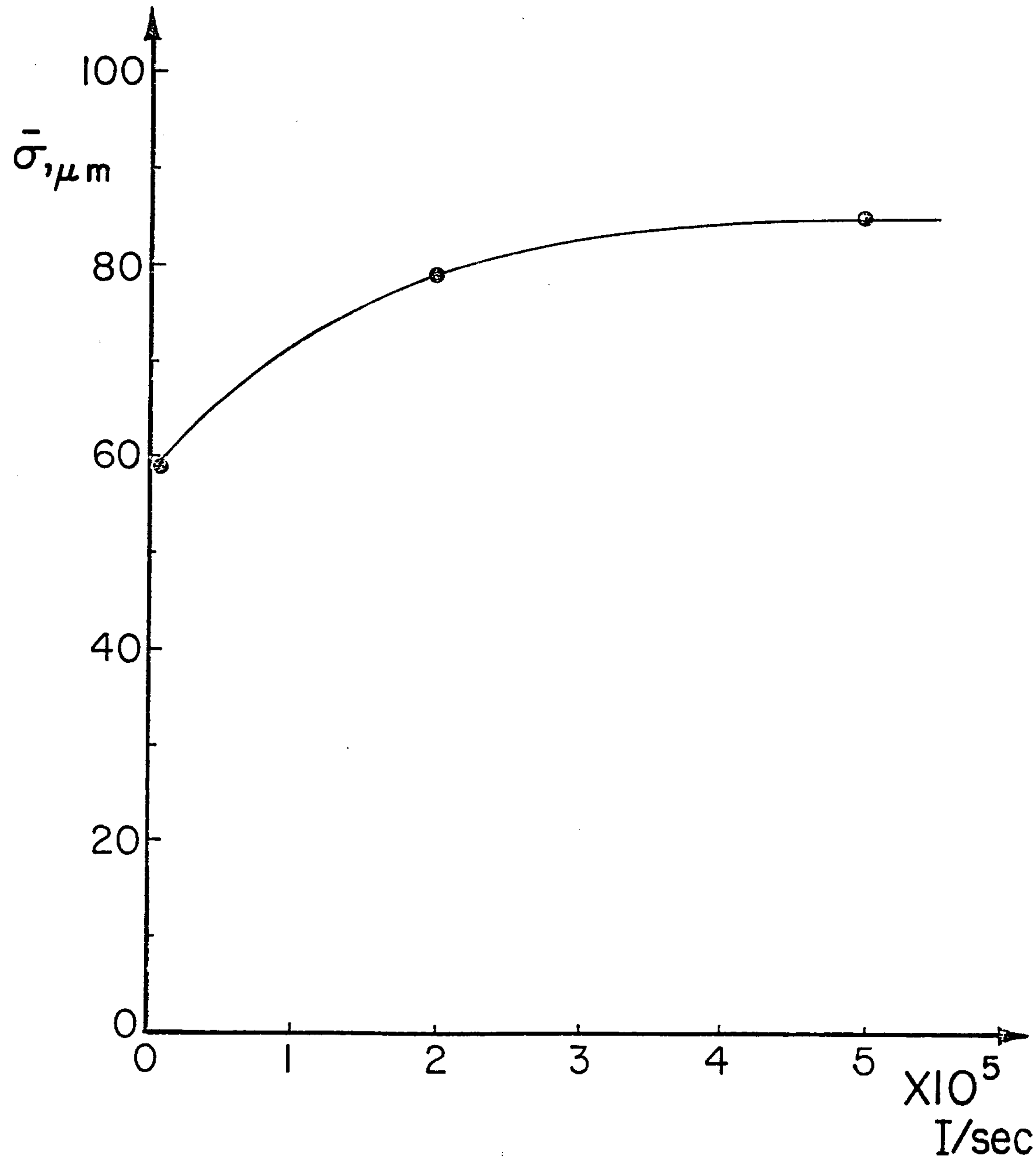

Fig. 6. Average spatial accuracy of drift chambers vs beam intensity.